Supplementary Material

Ursolic acid inhibits NF-κB signaling and attenuates MMP-9/TIMP-1 in progressive osteoarthritis: A network pharmacology-based analysis

Eman Maher Zahran[a*], Soad A. Mohamad[b], Mohamed M. Elsayed[c], Mohamed Hisham[d], Sherif A. Maher[e], Usama Ramadan Abdelmohsen[a,f], Mahmoud Elrehany[h], Samar Yehia Desoukey[f], Mohamed Salah Kamel[f]

[a]Department of Pharmacognosy, Faculty of Pharmacy, Deraya University, Universities Zone, New Minia City, 61111, Egypt. https://orcid.org/0000-0002-5517-082X.

[b]Department of Pharmaceutics and Clinical Pharmacy, Faculty of Pharmacy, Deraya University, Universities Zone, New Minia City, 61111, Egypt.

[c]Faculty of Pharmacy, Deraya University, Universities Zone, New Minia City, 61111, Egypt.

[d]Department of Pharmaceutical Chemistry, Faculty of Pharmacy, Deraya University, Universities Zone, New Minia City, 61111, Egypt

[e]Department of Biochemistry, Faculty of Pharmacy, New Valley University, New Valley, 72713, Egypt

[f]Department of Pharmacognosy, Faculty of Pharmacy, Minia University, 61519 Minia, Egypt

[g]Department of Pharmacognosy, College of Pharmacy, King Khalid University, Abha 62521, Saudi Arabia mrabeh@kku.edu.sa , Salshhri@kku.edu.sa

[h] Department of Biochemistry, Faculty of Pharmacy, Deraya University, Universities Zone, New Minia City, 61111, Egypt

***Corresponding author:** Eman Maher Zahran, emanzahran84@yahoo.com, eman.maher@deraya.edu.eg,

1. Metabolic profiling of n-hexane fraction of *Ocimum forskolei* and isolation of ursolic acid

LC-MS was carried out using a mass spectrometer of Synapt G2 HDMS quadrupole time-of-flight hybrid (Waters, Milford, CT, USA). A two ml of the sample was injected into a BEH C18 column (2.1 × 50 mm), which was optimized to 40° C, and then connected to the guard column. The gradient elution was employed, where the mobile phase consisted of purified water (A) and acetonitrile (B) containing 0.1% formic acid in each. The gradient program started with 10% B which was increased linearly in 30 min to 100% B at a flow rate of 300 µL/min and remained isocratic for 5 min before linearly decreasing to 10% B in 1 min. The injection volume was adjusted ~~at~~ to 10 µL, the tray temperature was maintained at 12° C with a total analysis time of 45 min. for each sample. High resolution mass spectrometry was carried out in both positive and negative ESI ionization modes with a spray voltage of 4.5 kV, a capillary temperature of 320° C and a mass range acquired at m/z from 150 to 1500. The MZmine 2.12 was employed for investigation of data, followed by converting the raw data into positive and negative files in mzML format with ProteoWizard. The compounds were then dereplicated and identified using the Dictionary of Natural Products (DNP) database [1].

The n-hexane fraction (400 mg) was subjected to VLC fractionation on a silica gel column using n-hexane-EtOAc gradient mixtures of increasing polarities (20, 30, 40, 50 and 100%). The effluents were collected in fractions which were concentrated to give four subfractions (II 1-II 4). Subfraction II 4 (70 mg) was subjected to silica gel column using DCM-MeOH gradient mixtures where a white powder was precipitated and purified. Then, it was dissolved in DMSO-d_6, at a concentration of 1 mg/500 µl of DMSO-$_6$, and subjected to ^{1}H-NMR analysis *via* a Brüker Avance, 400 MHz, NMR spectrometer, Germany), using Tetramethyl Silane (TMS) as a reference. This was followed by co-chromatography in comparison with an authentic ursolic acid sample obtained from pharmacognosy department, faculty of pharmacy, Deraya university. The run system used for TLC co-chromatography was DCM:Methanol 95:5 and the R_f values were measured.

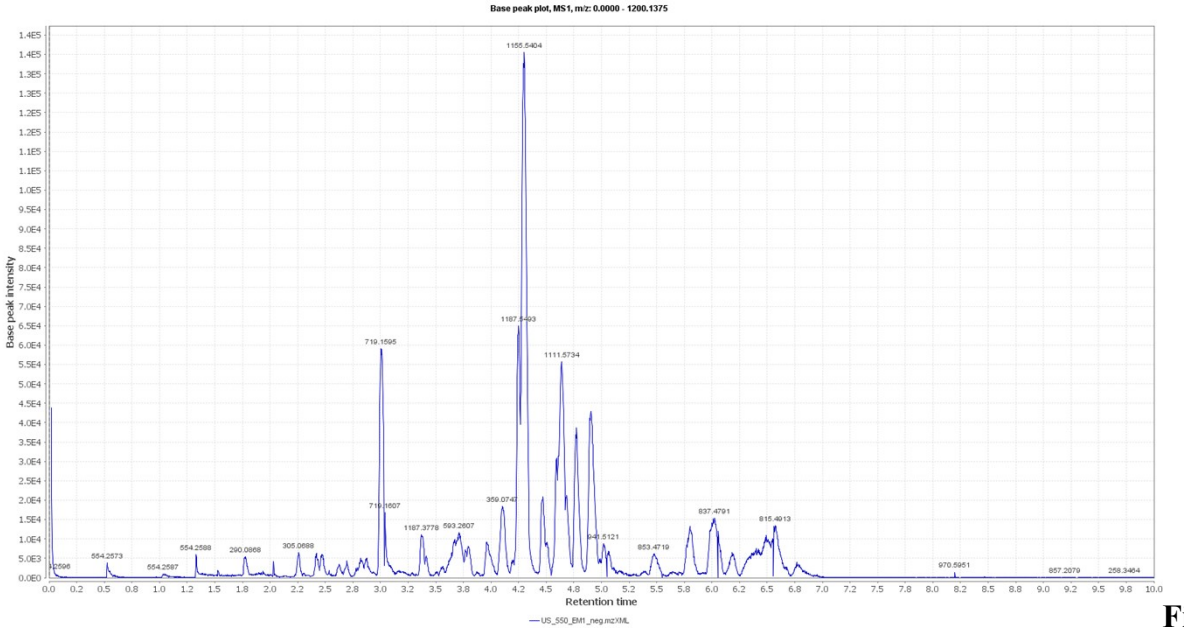

Figure S1: LC-HR-MS chromatogram of n-hexane fraction of *Ocimum forskolei*; negative mood

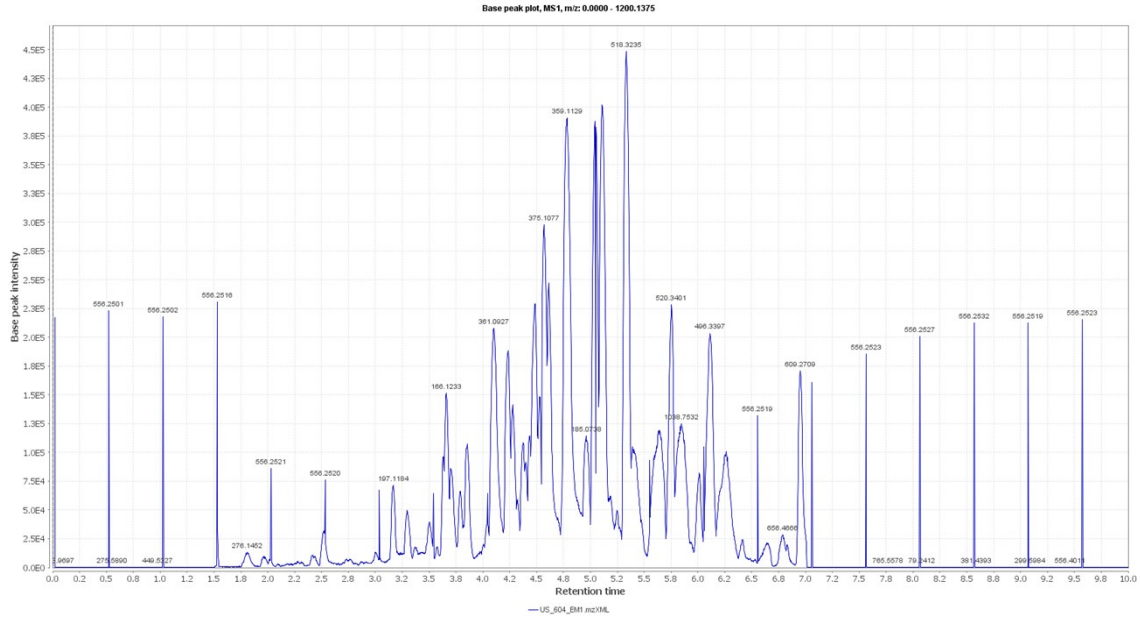

Figure S2: LC-HR-MS chromatogram of n-hexane fraction of *Ocimum forskolei*; positive mood

Table S1. Dereplicated metabolites from LC-HR-MS analysis of n-hexane fraction of *Ocimum forskolei*

No.	Compound	Acc. Mass g/mol	*m/z*	Mol. formula	Chemical class	Ref

1	4-hexenoic acid	114.07	114.011	$C_6H_{10}O_2$	Fatty acid	2
2	Fumaric acid	116.01	116.013	$C_4H_4O_4$	Fatty acid	3
3	Dihydroxybenzoic acid	154.03	153.011	C7H5O4	Phenolic compound	4
4	Eugenol	164.08	164.082	$C_{10}H_{12}O_2$	Phenolic compound	5
5	Vanillic acid	168.04	168.005	$C_8H_7O_4$	Phenolic compound	6
6	Ligustilidiol	224.10	224.104	$C_{12}H_{16}O_4$	Iridoid	7
7	12-hydroxy jasmonic acid	226.12	226.113	$C_{12}H_{18}O_4$	Cyclopenta-none derivative	8
8	Sacidumol A	236.10	236.104	C_{13}H16O4	Phenolic compound	9
9	Nigellicine	246.10	246.109	$C_{13}H_{14}N_2O_3$	Heterocyclic compound	10
10	2-Hydroxy-9,12,15-octadecatrienoic acid	294.46	294.467	$C_{18}H_{30}O_3$	Fatty acid	11
11	Sanguinone A	298.11	298.004	$C_{15}H_{14}N_4O_3$	Pyrrolo-quinoline alkaloid	12
12	Synparvolide C	300.12	300.120	$C_{14}H_{20}O_7$	Heterocyclic compound	13
13	Aegyptinone A	310.16	310.157	$C_{20}H_{22}O_3$	Heterocyclic compound	14
14	Scillascillin	312.06	312.062	$C_{17}H_{12}O_6$	Homoisoflavanone	15
15	Sahandone	324.21	324.187	$C_{21}H_{26}O_3$	Diterpene	16

16	5-O-Caffeoyl shikimic acid	336.08	336.084	$C_{16}H_{16}O_8$	Phenolic compound	17
17	5-O-p-Coumaroyl quinic acid	338.10	338.099	$C_{16}H_{18}O_8$	Phenolic compound	18
18	3-(3,4-Dihydroxyphenyl)-2-hydroxy propanoic acid	360.08	360.082	$C_{18}H_{16}O_8$	Phenolic compound	19
19	Ursolic acid	456.36	456.129	$C_{30}H_{48}O_3$	Triterpene	20

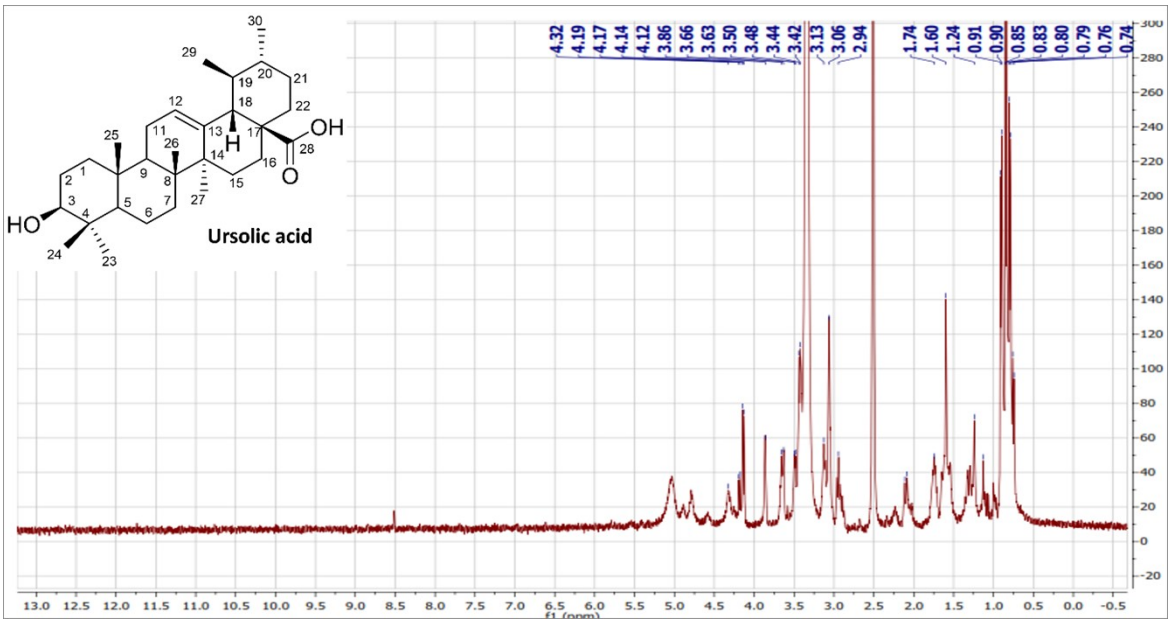

A

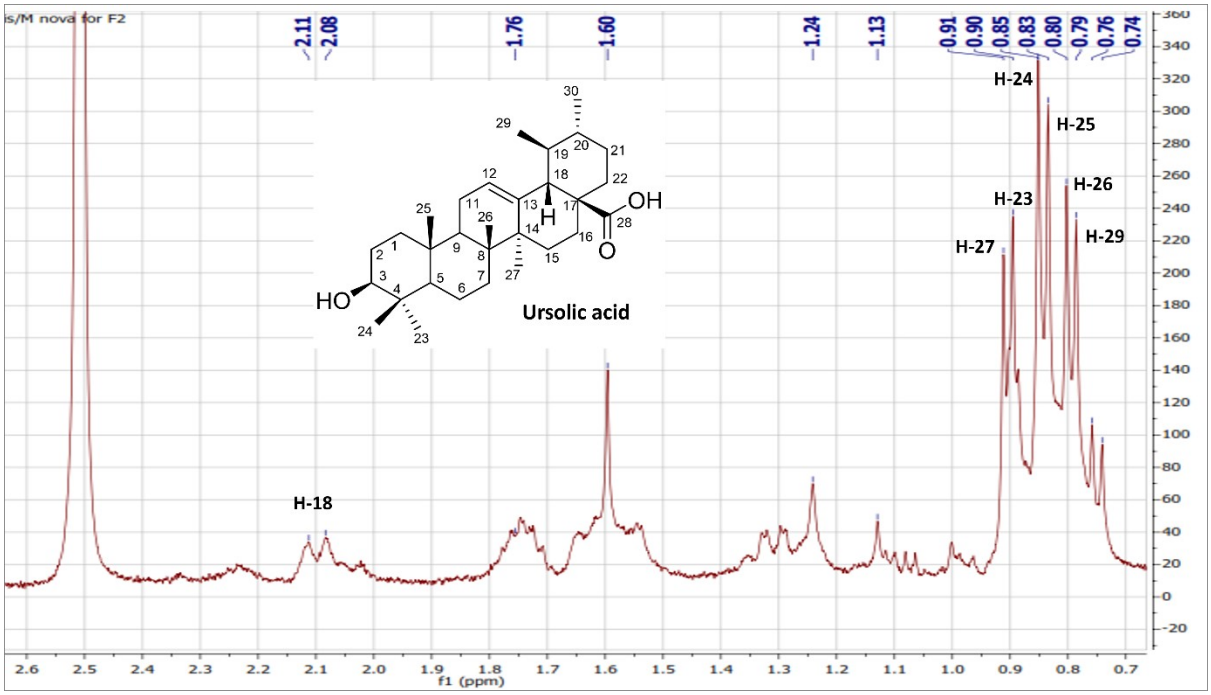

71

72 B

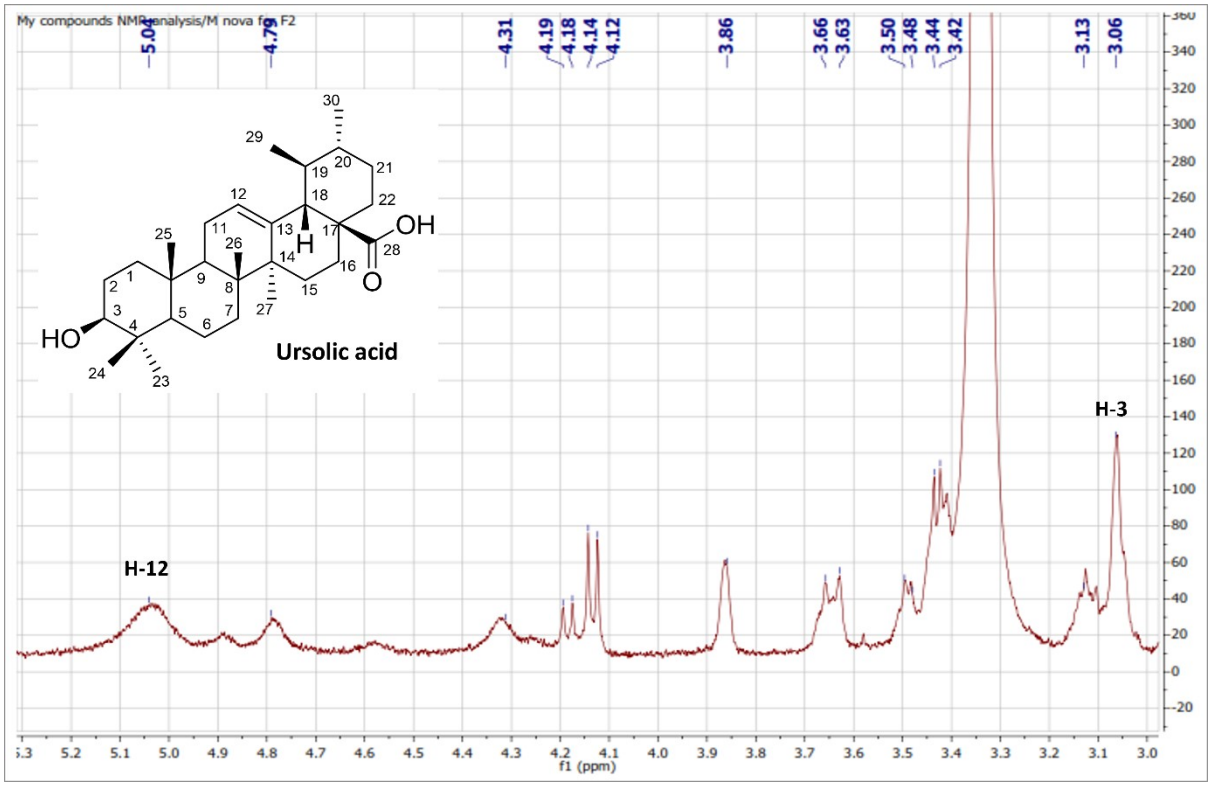

73

74 C

75 **Figure S3 A, B & C Integrated ^{1}H-NMR spectra of Ursolic acid (DMSO-d_6, 400 MHz)**

76 **Table S2. A list of ^{1}H-NMR chemical shifts of ursolic acid**

Assignment	Chemical shift δ_H	Integration, Multiplicity & *J* (Hz)
H-3	3.06	1H, s
H-12	5.04	1H, br s
H-18	2.10	1H, d, *J*= 11 Hz
H-23	0.90	3H, s, CH_3
H-24	0.85	3H, s, CH_3
H-25	0.83	3H, s, CH_3
H-26	0.80	3H, s, CH_3
H-27	0.91	3H, s, CH_3
H-29	0.79	3H, d, *J*= 6.4 Hz
H-30	0.85	3H, d, *J*= 6 Hz

2. Formulation of UA emulgel

Poloxamer, chitosan, PVA were purchased from Merck chemicals, USA. Ltd, Olive oil and lecithin from Sigma-Aldrich, USA, methanol from Sigma- Aldrich, Germany and glycerol from Ranbaxy laboratories Ltd. Three different formulations: UAE1, UAE2 and UAE3 were prepared by dissolving the defined amount of the drug in ethanol and lecithin then mixed with 5 ml of Olive oil, followed by addition of the surfactant and co-surfactant in well closed tubes for 24 hrs on magnetic stirrer at 200 rpm (75° C) and finally centrifugating the suspension at 5000 rpm (Figure S. Clear supernatant liquid was separated and filtered, then the absorbance was measured by a UV spectrophotometer (Shimadzu UV-1280, Japan) at 214 nm. The resulting emulsion was then cooled at room temperature by immersion in a thermostatic bath (10.0±0.1°C). [21, 22]

Table S3: Composition of different formulations of UA

Components	UA-E1	UA-E2	UA-E3
UA	2% w/w	2% w/w	2% w/w
Poloxamer	25% w/w	-	-
PVA	-	-	25% w/w
Chitosan (in 1% v/v glacial acetic acid)	-	25% w/w	-
Olive oil	20% w/w	20% w/w	20% w/w
Lecithin	7.5% w/w	7.5% w/w	7.5% w/w
Glycerol	2.5% w/w	2.5% w/w	2.5% w/w
Water	q.s. 100%	q.s. 100%	q.s. 100%

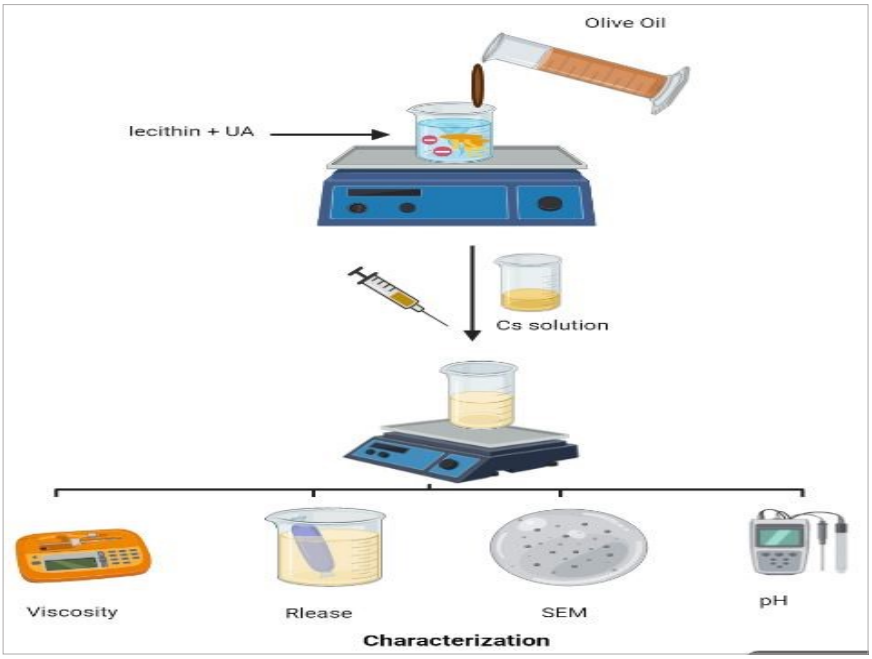

Figure S4: A schematic presentation for preparation steps of the emulgel

A B C

Figure S5. UA formulations: (A) UAE1, B) UAE2 and C) UA-E3

Table S4. physical examination of the three formulations

Formulation	Color	Odor	Grittiness	Phase separation	Homogeneity
Emulsion	White	pungent, fruity smell	-ve	None	Homogenous
UAE1	Light green	pungent, fruity smell	-ve	Slight	Homogenous
UAE2	White	pungent, fruity smell	-ve	None	Homogenous
UAE3	Dull light green	pungent, fruity smell	-ve	Separated	Slight

3. Characterization of the UA emulgel

The drug content (D.C.) was assessed based on the following equation:

- **Drug content** = $(C \times D.F \times V) \times C.F$ **……Equation 1**

Where; **C**, Concentration, **D.F**, Dilution factor, **V**, Volume taken and **C.F**, Conversion factor.

Additionally, 1 gram of each formulation was taken in a porous aluminum foil and placed separately in a 50 ml beaker containing 10 ml of 0.1 N NaOH, for measuring the swelling index (S) according to the equation:

$$S\% = \frac{W_t - W_0}{W_0} \times 100$$ ……**Equation 2**

W_t = Weight of swollen emulgel after time t, W_o = Original weight of emulgel at zero time.

Moreover, 0.25g of each formulation was enclosed in a dry test tube and observed over a temperature range of 2–50°C, where the temperature was changed gradually (5°C/h) to measure gelation temperature [23].

- **The bioadhesion measurement**

The bioadhesion measurement was performed using the modified Jolly balance method, to rationalize the mucoadhesion characteristics of the optimized emulgel [24], using the following equation:

$$\text{Bioadhesion force (N)} = \frac{Bioadhesive\ strength}{1000} \times 9.81$$ ……Equation 3

- **The centrifugation test**

In addition, the centrifugation test used to check the stability of the emulgel was performed by centrifugation of 5 g of UAE2 at 5000 rpm for 10 min at temperature of 25°C, then visually observing any signs of creaming or phase separation [25]. Besides, the globule size and ƹ-potential of all formulations were measured by zetasizer (Malvern zetasizer, 90) with the aid of a disposable sizing cuvette at 25.1°C, where 1 ml of the sample was diluted with 10 ml water and the results were recorded [24].

- **The permeation study**

As well, the modified Franz diffusion cell was used for permeation study, as reported [26]. where the mechanism of UA release from UAE2 was calculated according to the following kinetic models [27, 28]:

1. Zero order $R=K_0t$
2. First order: $R = 1 - e^{-k1}t$
3. Higuchi diffusion model: $Q = K^H \times t^{1/2}$

4. Baker–Lonsdale model: $3/2[1-(1-M_t/M_\infty)^{2/3}\ ]-M_t/M_\infty) = K_3 t$

5. Hixson–Crowell cube root law: $\frac{dW}{dt} = KC(C_s - C)$

6. Whereas R, Q or M_t/M_∞ refers to the fraction of drug released at time t, K, K_3 or K^H is the rate constant related to each model.

- **The scanning electron microscopy**

Finally, the morphology and dimensions of the inner oil phase of the UAE2 emulgel were evaluated by Field Emission Scanning Electron Microscopy (SEM) using an electron high tension of 5 and 15 kV as reported [29].

Table S5. Characterization of the three formulations

Formulation	Viscosity (Pa)	pH	Drug content (%)	Swelling index %	Gelation temperature (° C)	Bioadhesion strength (N)
UA emulsion	17±15	7.2±0.2	93.2±3	-	-	-
UA-E1	250±20	6.8±0.5	86.5±5	1.3±0.1	18±0.5	2.7±0.2
UA-E2	301±33	6±0.2	90±7	2±0.23	23±1	3.8±0.1
UA-E3	240±25	7±0.4	67±2	1.7±0.15	15±2	2.1±1

4. The analgesic assessment

The animals were grouped as previously prescribed and formulations were topically applied to the knee zone. A radiant heat source was used and the rats responses of leg withdrawal was timely recorded. The time from the start of heat application to leg withdrawal (in seconds) was taken as the leg withdrawal latency, determined immediately (0), at 5, 10, 15, 30, 45 and up to 60 min and repeated for five times (with an interval of 5 min) where the mean of five readings was recorded. The intensity of the heat source was fixed *via* a constant voltage-power supply and a maximum cut-off latency of 15 seconds was optimized to avoid skin damage, where the maximum possible analgesia (MPA) was calculated [30].

$$MPA = \frac{\text{Test reaction time - start reaction time}}{\text{15 - start reaction time}}$$

Table S6. Results of anti-inflammatory activity

Group	Knee joint diameter (mm)						
	Time 0	**30 m**	**1 h**	**2 h**	**4 h**	**6 h**	**8 h**
Control	7.22±0.09	7.31±0.07	7.38±0.05	7.8±0.15	8.18±0.12	8.78±0.16	9.3±0.06
Plain emulgel	7.85±0.05	7.96±0.09	8.04±0.12	8.33±0.06	8.47±0.06	8.77±0.15	9.31±0.11
UA-emugel	8.00±0.03	6.95±0.11	6.48±0.1	5.90±0.1	5.29±0.1	4.53±0.03	4.60±0.1
Algason	8.04±0.03	7.66±0.11	6.74±0.02	6.52±0.11	5.70±0.13	5.26±0.04	4.72±0.15

Each value represents the mean ± SD (N = 6). Statistical analysis were done by One-way ANOVA followed by the student's T-test (*P<0.05, **P<0.01, ***P<0.001).

Table S7. Results of analgesic activity:

Group	Basal reaction time (s)	Latency to reaction (s)			
		15 min	**30 m**	**45 m**	**60 m**
I	3.5±0.5	2.25±0.4	2.25±0.4	2.25±0.4	2.25±0.4
II	3.5±0.5	2.25±0.4	2.25±0.4	2.25±0.4	2.25±0.4
III	3.5±0.5	5±0.2	8.75±0.25	12.5±1	13.5±1

IV	3.5±0.5	4.75±1.7	6.25±0.4	8.75±0.4	8.75±0.7

160

161

162

163

164 **5. The local anaesthetic assessment**

165 **Table S8. Results of local anaesthetic activity:**

Gp	BRT (s)	Start of anasthesia (m)	Latency to Reaction(s)							
			At 1 m	**At 2 m**	**At 3 m**	**At 15 m**	**At 30 m**	**At 1 h**	**At 2 h**	**At 3 h**
I	1.5±0.5	-	1.5±0.5	1.5±0.5	1.5±0.5	1.5±0.5	1.5±0.5	1.5±0.5	1.5±0.5	1.5±0.5
II	1.5±0.5	-	1.5±0.5	1.5±0.5	1.5±0.5	1.5±0.5	1.5±0.5	1.5±0.5	1.5±0.5	1.5±0.5
III	1.5±0.5	1.5±0.5	3.5±0.5	5.0±0.2	5.5±0.5	7.8±0.8	8.5±0.3	13±0.7	13±0.7	15.5±0.2
IV	1.5±0.5	3.75±0.5	4.7±0.2	4.7±0.2	5.5	8±1	8±1	10.5±0.5	6.4±0.2	4.8±0.2

166 **BRT** refers to Basal reaction time.

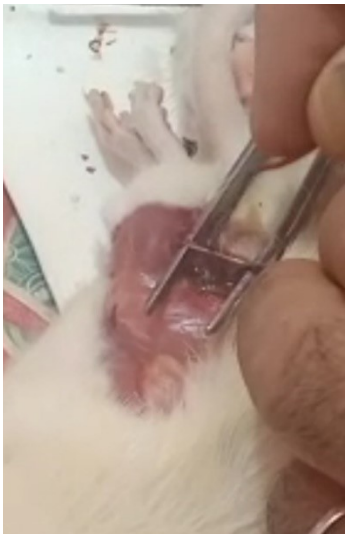

Figure S6. Sciatic nerve isolation and local anaethetic assessment

6. Network Pharmacology-Based Analysis of Ursolic Acid for Osteoarthritis

- **Collection of ursolic acid related targets from herbal databases**

he target genes were obtained through a search within the Traditional Chinese Medicine Systems Pharmacology Database and Analysis Platform (TCMSP) database (https://old.tcmsp-e.com/index.php) [31], BATMAN-TCM platform (http://bionet.ncpsb.org.cn/batman-tcm/) [32]. After that, and these target genes converted into their conical gene names using the UniProt database (https://www.uniprot.org/) [33].

- **Screening of wound healing process related target genes**

Genes associated with osteoarthritis process were collected from the GeneCards database (https://www.genecards.org/) [34] and Comparative Toxicogenomics Database (CTD) (http://ctdbase.org/) [35] databases using the keywords " Osteoarthritis " and the species limited to "Homo sapiens". Duplicate targets were removed, and overlapping component-related and disease-related proteins were identified based on interactivenn (http://www.interactivenn.net/) [36] intersections as potential targets of these components in osteoarthritis process.

- **Protein–Protein Interaction (PPI) Network Construction**

A PPI network with STRING version 12.0 (https://string-db.org/) [37] was produced using a query list of target genes and exported to Cytoscape software version 3.10.0 (USA) [38], a free

software package for visualizing, modeling, and analyzing molecular and genetic interaction networks (confidence score = 0.400) and the top 10 important genes were screened using the Cytohubba plug-in.

7. Molecular docking investigation

The X-ray crystallographic structure of TNF-α was co-crystallized with 6,7-Dimethyl-3-[(methyl(2-[methyl((1-[3-(trifluoromethyl)phenyl]-1*H*-indol-3-yl)methyl) amino]ethyl)-amino)methyl]-4*H*-chromen-4-one (PDB: 2AZ5, ligand ID: 307) obtained from the Protein Data Bank (https://www.rcsb.org/structure/2AZ5). The X-ray crystallographic structure of TGF-βR1 (PDB: 1VJY) was acquired from the protein data bank (https://www.rcsb.org/structure/1VJY) [39] and the native ligand naphthyridine (ligand ID: 460) was redocked into the protein.

Moreover, docking of UA against NF-κB protein active site (PDB: 1SVC) (https://www.rcsb.org/structure/1SVC) was performed [3]. Furthermore, docking against Voltage Gated Sodium Channel (VGSC) was also performed, where VGSC Nav 1.4-1 complex is one of the molecular targets for local anesthetics [40], which has been previously identified to have an active site as a cavity composed of four voltage-sensing domains (VSD-I to VSD-IV) with six segments for each domain and with a resolution of 3.2 A^{o} (PDB: 6AG) [41]. Regarding docking against Matrix Metalloproteinase-9 (MMP-9), the active site (PDB: 4XCT) was obtained from the protein data bank (https://www.rcsb.org/structure/4xct) [42].

Table S9: Molecular docking results and interacting residues for UA and co-crystallized ligand in TNF-α (PDB: 2AZ5), TGF-βR1 (PDB: 1VJY) and NF-κB (PDB: 1SVC) active site

Active site	Compound	Glide score (kcal/mol)	Glide energy (kcal/mol)	Interacting Residues	Type of Interaction
TNF-α (PDB: 2AZ5)	Ursolic acid	-2.85	-24.45	Leu120	H-bond
	Ligand 307	- 4.68	-46.29	Tyr 119	π-cation
TGF-βR1 (PDB: 1VJY)	Ursolic acid	-3.04	-40.10	Glu 228 Lys 342	2 H-bond H-bond, Salt bridge

	Ligand 460	-8.50	-70.12	His 283	H-bond
				Asp 351	H-bond
				Glu 245	Salt bridge
NF-κB pathway (PDB: 1SVC)	Ursolic acid	-3.36	-37.78	Lys 147	Salt bridge
				Lys 244	H-bond
	Dexamethasone	-4.16	-42.03	Lys 52	H-bond
				Gln 53	H-bond
				Leu 251	2 H-bond
				Glu 341	H-bond

209

210 **Table S10. Molecular docking results and interacting residues for UA and the co-**
211 **crystalized ligand (ID: N73) in MMP-9 (PDB: 4XCT) active site**

Active site	Compound	Glide score (kcal/mol)	Glide energy (kcal/mol)	Interacting Residues	Type of Interaction
MMP-9 (PDB : 4XCT)	Ursolic acid	-3.00	-34.52	Gln 405	H-bond
				Lys 1244	H-bond
	Ligand N73	- 6.30	-69.13	Leu 188	H-bond
				Ala 189	H-bond
				His 226	π-π stacking
				Zn 302	π-cation and metal coordination bond

212 **Table S11. Primers sequences used in qRT-PCR**

Primer	Genbank accession no.	Sequence 5' to 3'
IL-1β	NM_031512.2	Forward GTG ATG AAA GAC GGC ACA CC
		Reverse TCC TGG GGA AGG CAT TAG GA
TGF-β	NM_021578.2	Forward GCT GAA CCA AGG AGA CGG AA

		Reverse GAA GTT GGC ATG GTA GCC CT
TNF-α	NM_012675.3	Forward CCT CTC TGC CAT CAA GAG CC Reverse GGC TGG GTA GAG AAC GGA TG
NF-κB	NM_001276711.2	Forward CAG CAG ATG GCC CAT ACC TT Reverse CTG TCA TCC GTG CTT CCA GT
COX-2	NM_017232.4	Forward TTC GGG AGC ACA ACA GAG TG Reverse CAG CGG ATG CCA GTG ATA GA
MMP-9	NM_031055.2	Forward GCA TCT GTA TGG TCG TGG CT Reverse CGT GCG GGC AAT AAG AAA GG
TIMP-1	NM_053819.1	Forward CCT AGA GAC ACG CTA GAG CAG Reverse ACC GGA AAC CTG TGG CAT TT
GAPDH	NM_017008.4	Forward CTC TCT GCT CCT CCC TGT TC Reverse CGA CAT ACT CAG CAC CAG CA

References

1. E. M. Zahran, U. R. Abdelmohsen, A. Kolkeila, M. A. Salem, H. E. Khalil, S. Y. Desoukey, M. A. Fouad and M. S. Kamel, *Natural Product Research*, 2021, **35**, 5972-5976.
2. N. Babu, 2018.
3. N. Chirikova, D. Olennikov and A. Rokhin, *Chemistry of Natural Compounds*, 2008, **44**, 84-86.
4. D.-M.-C. Nguyen, D.-J. Seo, K.-Y. Kim, R.-D. Park, D.-H. Kim, Y.-S. Han, T.-H. Kim and W.-J. Jung, *Microbial Pathogenesis*, 2013, **59-60**, 52-59.
5. A. Suzuki, O. Shirota, K. Mori, S. Sekita, H. Fuchino, A. Takano and M. Kuroyanagi, *Chemical and Pharmaceutical Bulletin*, 2009, **57**, 245-251.
6. E. M. Zahran, U. R. Abdelmohsen, H. E. Khalil, S. Y. Desoukey, M. A. Fouad and M. S. Kamel, *Phytochemistry Reviews*, 2020, **19**, 907-953.
7. N. Z. Z. Mamadalieva, D. K. K. Akramov, L. A. A. Wessjohann, H. Hussain, C. Long, K. S. S. Tojibaev, E. Alshammari, M. L. L. Ashour and M. Wink, *Plants (Basel)*, 2021, **10**, 132.

8. A. Karioti, T. Milošević-Ifantis, N. Pachopos, N. Niryiannaki, D. Hadjipavlou-Litina and H. Skaltsa, *Journal of enzyme inhibition and medicinal chemistry*, 2015, **30**, 38-43.
9. Y. A. N. Y.-m. C. Y.-x. Li Xiao-zhen, *NATURAL PRODUCT RESEARCH AND DEVELOPMENT*, 2017, **29**, 183-189.
10. A. Hadipanah, M. Gheisari and A. Armin, *Scientia Agriculturae*, 2013, **4**, 55-57.
11. H. KÜHN, R. WIESNER, L. ALDER and T. SCHEWE, *European journal of biochemistry*, 1989, **186**, 155-162.
12. C. Garcia, C. Teodósio, C. Oliveira, C. Oliveira, A. Díaz-Lanza, C. Reis, N. Duarte and P. Rijo, *Current pharmaceutical design*, 2018, **24**, 4207-4236.
13. R. Pereda-Miranda, L. Hernández, M. J. Villavicencio, M. Novelo, P. Ibarra, H. Chai and J. M. Pezzuto, *Journal of Natural Products*, 1993, **56**, 583-593.
14. A. El-Lakany, *Natural Product Sciences*, 2003, **9**, 220-222.
15. B. Abegaz and H. Kinfe, *Natural Product Communications*, 2019, **14**, 1934578X1984581.
16. S. N. Ebrahimi, S. Zimmermann, J. Zaugg, M. Smiesko, R. Brun and M. Hamburger, *Planta medica*, 2013, **29**, 150-156.
17. M. Villalva, S. Santoyo, L. Salas-Pérez, M. d. l. N. Siles-Sánchez, M. Rodríguez García-Risco, T. Fornari, G. Reglero and L. Jaime, *Foods*, 2021, **10**, 2067.
18. Y. Yin, K. Zhang, L. Wei, D. Chen, Q. Chen, M. Jiao, X. Li, J. Huang, Z. Gong and N. Kang, *Frontiers in pharmacology*, 2021, **12**.
19. Y. Tang, M. Wang, X. Le, J. Meng, L. Huang, P. Yu, J. Chen and P. Wu, *Antioxidant and cardioprotective effects of Danshensu (3-(3, 4-dihydroxyphenyl)-2-hydroxy-propanoic acid from Salvia miltiorrhiza) on isoproterenol-induced myocardial hypertrophy in rats*, 2011.
20. M. Silva, I. Vieira, F. Mendes, I. Albuquerque, R. Santos, F. Silva and S. Morais, *Molecules (Basel, Switzerland)*, 2008, **13**, 2482-2487.
21. P. Nahak, G. Karmakar, P. Chettri, B. Roy, P. Guha, S. E. Besra, A. Soren, A. G. Bykov, A. V. Akentiev and B. A. J. L. Noskov, 2016, **32**, 9816-9825.
22. M. Gallarate, E. Mittone, M. E. Carlotti, M. Trotta, P. J. J. o. d. s. Piccerelle and technology, 2009, **30**, 823-833.
23. S. A. Fouad, E. B. Basalious, M. A. El-Nabarawi and S. A. Tayel, *International journal of pharmaceutics*, 2013, **453**, 569-578.
24. S. A. Mohamad, E. M. Zahran, M. R. Abdel Fadeel, A. Albohy and M. A. Safwat, *Int J Nanomedicine*, 2021, **16**, 1789-1804.
25. N. K. Thakur, P. Bharti, S. Mahant and R. Rao, *Scientia Pharmaceutica*, 2012, **80**, 1045-1060.
26. S. A. Mohamad, H. Salem, H. A. Yassin and H. F. Mansour, *Drug Design, Development and Therapy*, 2020, **14**, 4277.
27. M. Yu, Yuan, W., Li, D., Schwendeman, A., & Schwendeman, S. P. (2019). Predicting drug release kinetics from nanocarriers inside dialysis bags. Journal of Controlled Release, 315, 23-30..
28. M. P. Paarakh, Jose, P. A., Setty, C. M., & Christoper, G. P. (2018). Release kinetics–concepts and applications. Int J Pharm Res Technol, 8(1), 12-20..
29. E. M. Zahran, U. R. Abdelmohsen, A. T. Ayoub, M. A. Salem, H. E. Khalil, S. Y. Desoukey, M. A. Fouad and M. S. Kamel, *South African Journal of Botany*, 2020, **131**, 311-319.
30. J. R. Deuis, L. S. Dvorakova and I. Vetter, *Frontiers in Molecular Neuroscience*, 2017, **10**.
31. J. Ru, P. Li, J. Wang, W. Zhou, B. Li, C. Huang, P. Li, Z. Guo, W. Tao, Y. Yang, X. Xu, Y. Li, Y. Wang and L. Yang, *J Cheminform*, 2014, **6**, 13.
32. Z. Liu, F. Guo, Y. Wang, C. Li, X. Zhang, H. Li, L. Diao, J. Gu, W. Wang, D. Li and F. He, *Sci Rep*, 2016, **6**, 21146.
33. C. UniProt, *Nucleic Acids Res*, 2021, **49**, D480-D489.
34. S. Fishilevich, R. Nudel, N. Rappaport, R. Hadar, I. Plaschkes, T. Iny Stein, N. Rosen, A. Kohn, M. Twik, M. Safran, D. Lancet and D. Cohen, *Database (Oxford)*, 2017, **2017**.

35. A. P. Davis, T. C. Wiegers, J. Wiegers, B. Wyatt, R. J. Johnson, D. Sciaky, F. Barkalow, M. Strong, A. Planchart and C. J. Mattingly, *Toxicol Sci*, 2023, DOI: 10.1093/toxsci/kfad069.
36. H. Heberle, G. V. Meirelles, F. R. da Silva, G. P. Telles and R. Minghim, *BMC Bioinformatics*, 2015, **16**, 169.
37. D. Szklarczyk, R. Kirsch, M. Koutrouli, K. Nastou, F. Mehryary, R. Hachilif, A. L. Gable, T. Fang, N. T. Doncheva, S. Pyysalo, P. Bork, L. J. Jensen and C. von Mering, *Nucleic Acids Res*, 2023, **51**, D638-D646.
38. P. Shannon, A. Markiel, O. Ozier, N. S. Baliga, J. T. Wang, D. Ramage, N. Amin, B. Schwikowski and T. Ideker, *Genome Res*, 2003, **13**, 2498-2504.
39. F. Gellibert, J. Woolven, M. H. Fouchet, N. Mathews, H. Goodland, V. Lovegrove, A. Laroze, V. L. Nguyen, S. Sautet, R. Wang, C. Janson, W. Smith, G. Krysa, V. Boullay, A. C. De Gouville, S. Huet and D. Hartley, *J Med Chem*, 2004, **47**, 4494-4506.
40. E. M. Zahran, U. R. Abdelmohsen, M. M. Shalash, M. A. Salem, H. E. Khalil, S. Y. Desoukey, M. A. Fouad, M. Krischke, M. Mueller and M. S. Kamel, *Natural product research*, 2020, 1-7.
41. X. Pan, Z. Li, Q. Zhou, H. Shen, K. Wu, X. Huang, J. Chen, J. Zhang, X. Zhu and J. J. S. Lei, 2018, **362**.
42. E. Nuti, A. R. Cantelmo, C. Gallo, A. Bruno, B. Bassani, C. Camodeca, T. Tuccinardi, L. Vera, E. Orlandini and S. J. J. o. m. c. Nencetti, 2015, **58**, 7224-7240.